

## On the Origin of Cis Selectivity in the Cyclization of N-Protected 2-Substituted 3-Aza-5-hexenyl Radicals: A Density Functional Study

David Shanks, Stefan Berlin, Magnus Beşev, Henrik Ottosson,\* and Lars Engman\*

Department of Organic Chemistry, Institute of Chemistry, Box 599, Uppsala University, 751 24, Uppsala, Sweden

*lars.engman@kemi.uu.se; henrik.ottosson@kemi.uu.se*

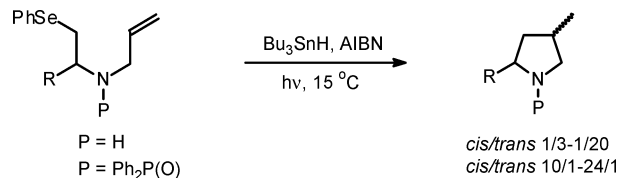
Received September 23, 2003

Cyclization of the *N*-dimethylphosphinoyl-2-methyl-3-aza-5-hexenyl radical has been studied at the UB3LYP/6-31+G(d)//UB3LYP/6-31G(d) hybrid density functional level. The corresponding radical precursor has been synthesized and found to give *cis/trans* ratios of up to 10/1 in reductive radical cyclizations. The relative energies of reactant and transition state conformers were determined. In discord with the Beckwith–Houk model, it has been found that chair-axial transition states, which lead to *cis* products, are lowest in energy, rationalizing the observed experimental diastereoselectivity.

### Introduction

Due to rapid progress in the field of radical chemistry during the last three decades, radical carbon–carbon bond formation<sup>1</sup> is nowadays routinely considered in retrosynthetic analysis. Although the chemo- and regioselectivity of radical reactions are often good, high levels of stereocontrol can often be difficult to achieve.<sup>2</sup> For acyclic stereoselection, significant levels of diastereoselection have been observed in radical addition and reduction reactions using preexisting chiral centers, chiral auxiliaries, or chiral Lewis acids. Attempts to control diastereoselectivity in cyclization reactions have so far been less successful. Selectivity is governed primarily by conformational and steric effects as described by the Beckwith–Houk transition state model for 5- and 6-exo cyclization.<sup>3</sup> However, the diastereoselectivity in simple systems rarely exceeds 4:1 in favor of the major diastereomer. Recent successful strategies to perturb Beckwith–Houk diastereoselectivities in intramolecular radical cyclization

### SCHEME 1



reactions are based on Lewis acid coordination<sup>4</sup> or the stereochemical influence of the anomeric effect.<sup>5</sup> Some time ago, we found that diastereoselectivity in the cyclization of 2-substituted 3-aza-5-hexenyl radicals was critically dependent on the *N*-substituent.<sup>6</sup> Thus, whereas *N*-unprotected derivatives afforded *trans*-2,4-disubstituted pyrrolidines with fair to good selectivity, an *N*-diphenylphosphinoyl group directed cyclization to occur in a highly *cis* selective manner (Scheme 1).

Quantum chemical calculations, and density functional theory (DFT) calculations in particular, have proved to be of utility in understanding the selectivity in radical cyclizations.<sup>7</sup> DFT has become the method of choice for

(1) Giese, B. *Radicals in Organic Synthesis: Formation of C–C Bonds*; Pergamon Press: Oxford, 1986. Regitz, M.; Giese, B., Eds. *Houben-Weyl, Methoden der Organischen Chemie*; Georg Thieme Verlag: Stuttgart; Band E19a. Curran, D. P. In *Comprehensive Organic Synthesis*; Trost, B. M., Fleming, I., Semmelhack, M. F., Eds.; Pergamon Press: Oxford, 1991; Vol 4, p 715 and 779. Motherwell, W. B.; Crich, D. *Free Radical Chain Reactions in Organic Synthesis*; Academic Press: New York, 1992. Fossey, J.; Lefort, D.; Sorba, J. *Free Radicals in Organic Chemistry*; Wiley: New York, 1995. Giese, B.; Kopping, B.; Göbel, T.; Dickhaut, J.; Thoma, G.; Kulicke, K. J.; Trach, F. *Org. React.* **1996**, *48*, 301. Parsons, A. F. *An Introduction to Free Radical Chemistry*; Blackwell Science: Oxford, 2000. Renaud, P.; Sibi, M. P., Eds. *Radicals in Organic Synthesis*; Wiley-VCH: Weinheim, 2001; Vols. 1 and 2.

(2) Curran, D. P.; Porter, N. A.; Giese, B. *Stereochemistry of Radical Reactions—Concepts, Guidelines and Synthetic Applications*; VCH: New York, 1996.

(3) Beckwith, A. L. J.; Easton, C. J.; Serelis, A. K. *J. Chem. Soc., Chem. Commun.* **1980**, 482. Beckwith, A. L. J.; Lawrence, T.; Serelis, A. K. *J. Chem. Soc., Chem. Commun.* **1980**, 484. Beckwith, A. L. J.; Schiesser, C. H. *Tetrahedron* **1985**, *41*, 3925. Spellmeyer, D. C.; Houk, K. N. *J. Org. Chem.* **1987**, *52*, 959.

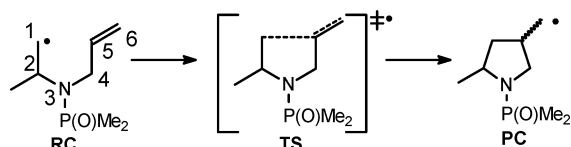
(4) Ericsson, C.; Engman, L. *Org. Lett.* **2001**, *3*, 3459. Renaud, P.; Andrau, L.; Schenk, K. *Synlett* **1999**, 1462. Delouvrié, B.; Fensterbank, L.; Lacôte, E.; Malacria, M. *J. Am. Chem. Soc.* **1999**, *121*, 11395. Molander, G. A.; McWilliams, J. C.; Noll, B. C. *J. Am. Chem. Soc.* **1997**, *119*, 1265. Sibi, M. P.; Ji, J. *J. Am. Chem. Soc.* **1996**, *118*, 3063. Nishida, M.; Ueyama, E.; Hayashi, H.; Ohtake, Y.; Yamaura, Y.; Yanaginuma, E.; Yonemitsu, O.; Nishida, A.; Kawahara, N. *J. Am. Chem. Soc.* **1994**, *116*, 6455. Feldman, K. S.; Romanelli, A. L.; Ruckle, Jr, R. E.; Jean, G. *J. Org. Chem.* **1992**, *57*, 100. For a general review on the use of Lewis acids in free radical reactions, see: Renaud, P.; Gerster, M. *Angew. Chem., Int. Ed.* **1998**, *37*, 2562.

(5) Villar, F.; Kolly-Kovak, T.; Equey, O.; Renaud, P. *Chem. Eur. J.* **2003**, *9*, 1566. Villar, F.; Renaud, P. *Tetrahedron Lett.* **1998**, *39*, 8655. Beckwith, A. L. J.; Page, D. M. *J. Org. Chem.* **1998**, *63*, 5144.

(6) Beşev, M.; Engman, L. *Org. Lett.* **2000**, *2*, 1589.

(7) For some recent examples of cyclizations calculated using DFT, see: Sung, K.; Wang, Y. Y. *J. Org. Chem.* **2003**, *68*, 2771. Fang, X.; Xia, H.; Yu, H.; Dong, X.; Chen, M.; Wang, Q.; Tao, F.; Li, C. *J. Org. Chem.* **2002**, *67*, 8481. Falzon, C. T.; Ryu, I.; Schiesser, C. H. *Chem. Commun.* **2002**, 2338.

## SCHEME 2



radical chemists due to its inherent handling of electron correlation, lower spin contamination, and relative cost-effectiveness in comparison to correlated Hartree–Fock-based methods such as second-order Møller–Plesset theory (MP2). Therefore, we decided to undertake a computational investigation into the origin of diastereoselectivity in an *N*-protected 2-substituted 3-aza-5-hexenyl radical cyclization. To minimize the size of the computational system and limit the number of possible conformers, model reaction RC (reactant conformer) → PC (product conformer) (Scheme 2), which has an *N*-dimethylphosphinoyl group and a 2-methyl substituent, was chosen for calculation.

First, however, it was decided to synthesize the corresponding radical precursor **3** and study the diastereoselectivity of its radical cyclization in comparison with the systems already investigated.

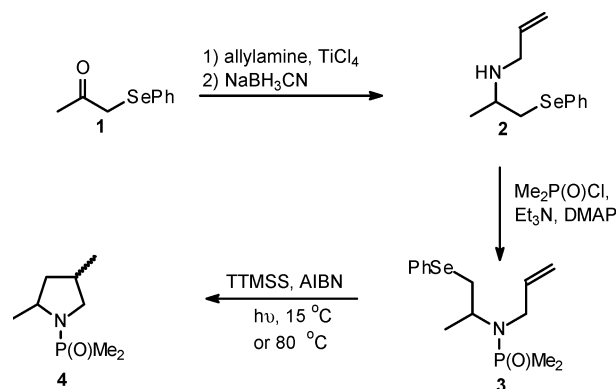
## Computational Details

All calculations were carried out with the Gaussian 98 program package.<sup>8</sup> Reactant (RC) and transition-state (TS) geometries were optimized using the B3LYP hybrid-DFT method of Becke,<sup>9</sup> together with the 6-31G(d) basis set of Pople and co-workers.<sup>10</sup> The unrestricted formalism was used, and spin contamination was low along the reaction paths ( $\langle S^2 \rangle < 0.784$ ). Frequency calculations were performed on all stationary points at the UB3LYP/6-31G(d) level of computation in order to obtain corrections for the zero-point energies (ZPEs) and to ascertain that the computed transition states were first-order saddle points. Finally, because diffuse functions were recently found to be more important in DFT calculations than in calculations using wave function-based approaches,<sup>11</sup> we carried out single-point energy calculations with the 6-31+G(d) basis set. The UB3LYP/6-31+G(d)//UB3LYP/6-31G(d) energies, with ZPE corrections, scaled by a factor of 0.9806,<sup>12</sup> are reported.

## Results and Discussion

**Synthesis.** The radical precursor **3** was synthesized by subjecting phenylselenenylacetone (**1**) to reductive

## SCHEME 3



T (°C)	Yield (%)	cis/trans
15	74	10/1
80	65	4/1

amination with allylamine,<sup>6</sup> followed by dimethylphosphinoylation of the resulting secondary amine **2** (Scheme 3). Reductive radical cyclization of selenide **3** at 15 °C using TTMSS/AIBN under UV irradiation gave pyrrolidine **4** in 74% yield and a cis/trans ratio of 10/1. Thermolytic conditions (heating at reflux in benzene) gave both a lower yield (65%) and a poorer cis/trans ratio (4/1). Although, as could be expected, the diastereomeric ratio was not as good as that obtained using the diphenylphosphinoyl protecting group (18/1),<sup>6</sup> the cyclization was still largely cis selective, and with these encouraging results in hand, we proceeded with calculations.

**Calculations.** The reactant (RC) and transition state (TS) conformations identified were named chair-axial, chair-equatorial, boat-axial, boat-equatorial, *cis*-twist-axial, and *trans*-twist-axial depending on the relative spatial arrangement of C<sup>1</sup>–C<sup>2</sup>–N–C<sup>4</sup>–C<sup>5</sup>–C<sup>6</sup> (Scheme 2) and whether the methyl substituent adopted a pseudo-equatorial or pseudoaxial position in the transition state. The reactant conformers are named in accordance with the corresponding transition state but do not necessarily bear similarity to this conformation (Figure 1).

Each conformation was found to have four rotational isomers around the P–N bond, which were further labeled with the terms *gauche*(+), *gauche*(–), *syn*-eclipsed, or *anti*-eclipsed depending on the O=P–N–C<sup>2</sup> dihedral angle of the reactant conformer. This finding was surprising because it would be anticipated that eclipsed conformations are energetically unfavorable. The eclipsed rotamers are, however, on average 1.2 kcal/mol more stable than the *gauche* rotamers, suggesting that the P=O bond conjugates to the nitrogen lone pair in the eclipsed conformations. The P–N bond length is ~0.01 Å shorter in the eclipsed rotamers, and the mean deviation of the nitrogen atom from planarity, measured using the P–N–C<sup>2</sup>–C<sup>4</sup> improper torsion angle, is only 15.7° compared to 30.4° for the *gauche* rotamers, providing strong evidence of O=P–N conjugation.

Interestingly, despite extensive searching, *anti*-eclipsed-boat-equatorial, *anti*-eclipsed-chair-equatorial, and *syn*-eclipsed-boat-axial transition states could not be located. Instead, starting structures resembling these proposed transition states invariably collapsed to the twist-axial structures **TS-8**, **TS-12**, and **TS-15** upon optimization

(8) Frisch, M. J.; Trucks, G. W.; Schlegel, H. B.; Scuseria, G. E.; Robb, M. A.; Cheeseman, J. R.; Zakrzewski, V. G.; Montgomery, J. A., Jr.; Stratmann, R. E.; Burant, J. C.; Dapprich, S.; Millam, J. M.; Daniels, A. D.; Kudin, K. N.; Strain, M. C.; Farkas, O.; Tomasi, J.; Barone, V.; Cossi, M.; Cammi, R.; Mennucci, B.; Pomelli, C.; Adamo, C.; Clifford, S.; Ochterski, J.; Petersson, G. A.; Ayala, P. Y.; Cui, Q.; Morokuma, K.; Malick, D. K.; Rabuck, A. D.; Raghavachari, K.; Foresman, J. B.; Cioslowski, J.; Ortiz, J. V.; Stefanov, B. B.; Liu, G.; Liashenko, A.; Piskorz, P.; Komaromi, I.; Gomperts, R.; Martin, R. L.; Fox, D. J.; Keith, T.; Al-Laham, M. A.; Peng, C. Y.; Nanayakkara, A.; Gonzalez, C.; Challacombe, M.; Gill, P. M. W.; Johnson, B. G.; Chen, W.; Wong, M. W.; Andres, J. L.; Head-Gordon, M.; Replogle, E. S.; Pople, J. A. *Gaussian 98*, revision A.9; Gaussian, Inc.: Pittsburgh, PA, 1998.

(9) Becke, A. D. *J. Chem. Phys.* **1993**, *98*, 5648. Stephens, P. J.; Devlin, F. J.; Chabalowski, C. F.; Frisch, M. J. *J. Phys. Chem.* **1994**, *98*, 11623.

(10) Hariharan, P. C.; Pople, J. A. *Theo. Chim. Acta* **1973**, *28*, 213.

(11) Lynch, B. J.; Zhao, Y.; Truhlar, D. G. *J. Phys. Chem. A* **2003**, *107*, 1384.

(12) Scott, A. P.; Radom, L. *J. Phys. Chem.* **1996**, *100*, 16502.

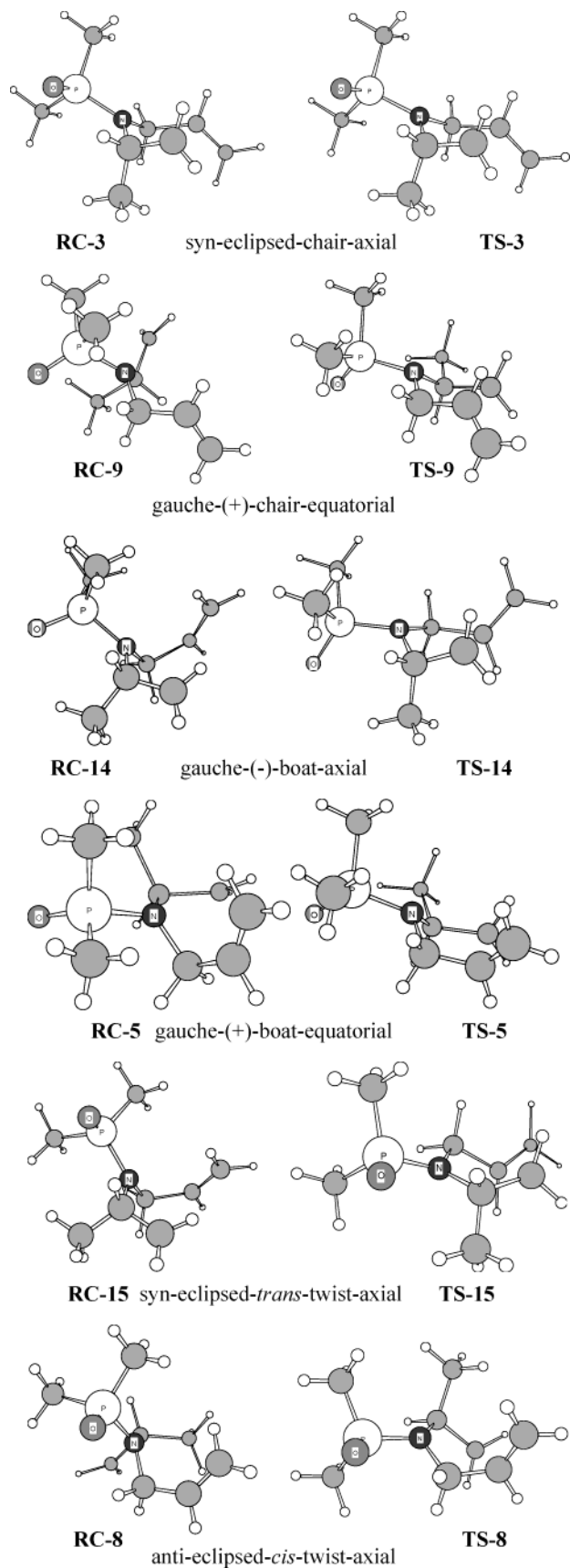


**FIGURE 1.** Lowest energy transition states of representative conformations (right) and their corresponding reactant conformers (left).

**TABLE 1.** Relative UB3LYP/6-31G+(d)//UB3LYP/6-31G(d) + ZPE Energies of Reactant Conformers and Transition States for the 5-Exo Cyclization of the N-dimethylphosphinoyl-2-methyl-3-aza-5-hexenyl Radical<sup>a</sup>

conformer	label	RC	TS
gauche-(+)-chair-axial	<b>1</b>	1.6	5.5
gauche(-)-chair-axial	<b>2</b>	1.6	5.3
syn-eclipsed-chair-axial	<b>3</b>	0.0	4.4
anti-eclipsed-chair-axial	<b>4</b>	0.1	5.1
gauche-(+)-boat-equatorial	<b>5</b>	5.2	10.1
gauche(-)-boat-equatorial	<b>6</b>	2.5	11.8
syn-eclipsed-boat-equatorial	<b>7</b>	1.7	11.8
anti-eclipsed-cis-twist-axial	<b>8</b>	1.6	9.4
gauche-(+)-chair-equatorial	<b>9</b>	1.7	7.6
gauche(-)-chair-equatorial	<b>10</b>	1.8	8.6
syn-eclipsed-chair-equatorial	<b>11</b>	1.2	8.6
anti-eclipsed-trans-twist-axial	<b>12</b>	0.3	7.1
gauche-(+)-boat-axial	<b>13</b>	2.0	8.3
gauche(-)-boat-axial	<b>14</b>	1.4	7.2
syn-eclipsed-trans-twist-axial	<b>15</b>	0.9	6.0
anti-eclipsed-boat-axial	<b>16</b>	2.5	7.4

<sup>a</sup> Energies are in kcal/mol. **RC-3** is taken as a reference.

(Figure 1). Twist transition states in 5-*exo*-trig radical cyclizations have recently been discovered by the groups of Schiesser<sup>13</sup> and Houk.<sup>14</sup> Those findings and the work presented herein (*vide infra*) demonstrate the importance of considering these transition states in rationalizing or predicting the outcome of 5-*exo* radical cyclizations.

Energies for all reactant conformers and transition states are collected in Table 1. Entries **1–8** lead to *cis* products and entries **9–16** to *trans* products (Figure 2). The lowest energy reactant conformers, **RC-3** and **RC-4**, have relative energies of 0.0 kcal/mol and 0.1 kcal/mol respectively, and both lead to the *cis* product. The lowest energy reactant conformer leading to the *trans* product, **RC-12**, has a relative energy of 0.3 kcal/mol, showing that at the reactant state there is a very slight bias toward conformers leading to the *cis* product. However, this bias is substantially more pronounced when considering the relative energies of the transition states. The lowest energy transition state leading to the *cis* product is **TS-3**, with a relative energy of 4.4 kcal/mol. The lowest energy transition state leading to the *trans* product is **TS-15**, which lies ~1.6 kcal/mol higher in energy. The difference between the calculated Gibbs free energies of these two transition states at room temperature is ~1.4 kcal/mol, which would correspond to a *cis/trans* ratio of 11/1, assuming the reaction is under kinetic control. This is in reasonable agreement with the experimental value of 10/1.

In discord with the Beckwith–Houk model, the chair-equatorial transition states lie between 2.1 and 4.3 kcal/mol higher in energy than those of the chair-axial conformations. This is due to A<sup>1,2</sup> strain between the dimethylphosphinoyl group and the pseudoequatorial methyl substituent.<sup>15</sup> The boat transition states lie 1.5–4.1 kcal/mol higher than their chair counterparts. This

(13) Corminboeuf, O.; Renaud, P.; Schiesser, C. H. *Chem. Eur. J.* **2003**, *9*, 1578.

(14) Leach, A. G.; Wang, R.; Wohlhieter, G. E.; Khan, S. I.; Jung, M. E.; Houk, K. N. *J. Am. Chem. Soc.* **2003**, *125*, 4271.

(15) Hopman, J. C. P.; van den Berg, E.; Ollero, L. O.; Hiemstra, H.; Speckamp, W. N. *Tetrahedron Lett.* **1995**, *36*, 4315. Craig, D.; Meadows, J. D.; Pecheux, M. *Tetrahedron Lett.* **1998**, *39*, 147.

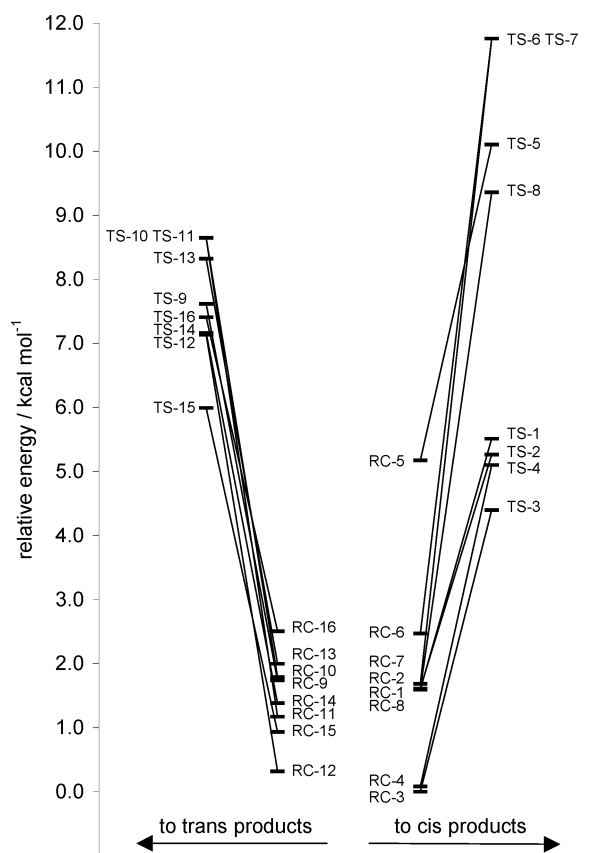


**FIGURE 2.** UB3LYP/6-31+G(d)//UB3LYP/6-31G(d) + ZPE energies (kcal/mol) for conformers leading to cis (right) and trans (left) products.

means that the chair-axial conformations are lowest in energy, and the boat-equatorial ones are highest. Therefore, it is apparent that the chair-axial pathway will be dominant for the production of the major cis product. The favored pathway hangs more finely in the balance for the minor trans product, since the reactants and transition states of most conformations are similar in energy. The *trans*-twist-axial transition state (TS-15) is, however, significantly lower in energy, and it is therefore probable that this pathway will be the most significant contributor to formation of the trans product.

The  $A^{1,2}$  strain experienced by transition states with a pseudoequatorial methyl group leads to the corresponding reactant conformations distorting from a typical chair or boat arrangement by rotation around the N–C<sup>2</sup> bond. This results in these reactant conformers having a much longer bond-forming (C<sup>1</sup>–C<sup>5</sup>) distance than those with an axial methyl substituent. Thus, the chair-axial, boat-axial, and twist-axial reactant conformers have an average distance of 2.99, 3.42, and 3.62 Å, respectively, compared to the chair-equatorial and boat-equatorial conformers, which have average distances of 3.84 and 3.86 Å. This trend vanishes for the transition states, where chair-axial, boat-axial, twist-axial, chair-equatorial, and boat-equatorial conformers now have average distances of 2.30, 2.32, 2.33, 2.32, and 2.33 Å, respectively. However, when comparing transition-state energies, it can be seen that on going from reactant conformer to transition state, the increasing degree of constraint on the bond-forming distance is paid for in increased

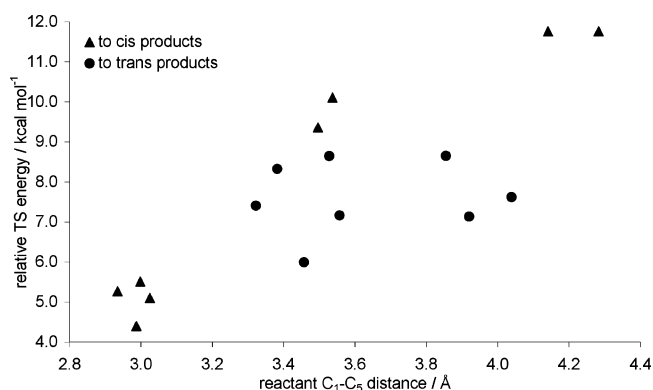


**FIGURE 3.** Transition-state energy vs distance between bond-forming carbons in the reactant conformer.

strain (Figure 3). This rationalizes the results from previous studies,<sup>6</sup> which show that bulky C<sup>2</sup> substituents increase the cis selectivity. It can also be surmised that larger alkyl substituents on the phosphinoyl protecting group, such as *tert*-butyl groups, should further increase the cis selectivity.

## Conclusion

Density functional calculations have been used to rationalize the cis selectivity in 5-*exo* cyclization of N-protected 3-aza-5-hexenyl radicals. It was calculated that both reactant and transition-state conformers leading to the cis products were lower in energy compared to conformers leading to trans products. In discord with the Beckwith–Houk model, conformers with a pseudoequatorial substituent were lower in energy than those with a pseudoequatorial substituent due to unfavorable  $A^{1,2}$  strain in the latter. This leads to the possibility of designing reactions in the future which are even more cis selective by variation of the N-protecting group.

## Experimental Section

**N-Allyl-N-dimethylphosphinoyl-2-aminopropyl Phenyl Selenide (3).** DMAP (26 mg, 0.11 mmol) and Et<sub>3</sub>N (164 μL, 1.18 mmol) were added to a stirred solution of *N*-allyl-2-aminopropyl phenyl selenide **2** (150 mg, 0.59 mmol) in dry CH<sub>2</sub>Cl<sub>2</sub> (10 mL) under N<sub>2</sub>. The mixture was cooled to 0 °C, after which dimethylphosphinic chloride (133 mg, 1.18 mmol) was added. The mixture was then stirred overnight. After in vacuo removal of solvent, the residue was purified by flash chromatography to afford the title compound **3** (148 mg, 76%): <sup>1</sup>H NMR (CDCl<sub>3</sub>) δ 1.34 (d, *J* = 6.7, 3H), 1.40 (dq, *J* = 11.4, 0.7, 3H), 1.43 (dq, *J* = 11.4, 0.7, 3H), 2.96 (dd, *J* = 12.3, 8.0, 1H), 3.18 (dd, *J* = 6.6, 12.3, 1H), 3.50–3.65 (several multiplets, 2H), 3.71 (m, 1H), 5.09 (dq, *J* = 10.1, 1.5, 1H), 5.18 (dq, *J* = 17.1, 1.5, 1H), 5.84 (dddd, *J* = 5.6, 6.2, 10.1, 17.1, 1H), 7.24–7.28 (several multiplets, 3H), 7.50–7.54 (several multiplets, 2H); <sup>13</sup>C NMR (CDCl<sub>3</sub>) δ 15.5 (d, *J* = 45), 16.4 (d, *J* = 45), 19.8 (2 signals), 34.3 (2 signals), 44.4 (2 signals), 51.8 (2 signals), 116.3, 127.0, 129.2, 130.0, 132.8, 138.0.

**N-Dimethylphosphinoyl-2,4-dimethylpyrrolidine (4).** AIBN (10 mg, 0.06 mmol) and TTMSS (224 μL, 0.73 mmol) were added to a stirred solution of selenide **3** (200 mg, 0.61 mmol) in benzene (20 mL) under N<sub>2</sub>. The solution was either irradiated in a micro photochemical reaction assembly (*T* = 15 °C) or refluxed (*T* = 80 °C) overnight. After removal of solvent in vacuo and subsequent purification by flash chromatography, the title compound **4** (*T* = 15 °C; 78 mg, 74%, cis/trans 10/1; *T* = 80 °C; 69 mg, 65%, cis/trans 4/1) was

obtained as a mixture of cis and trans isomers. **(4, cis):**  $^1\text{H}$  NMR ( $\text{CDCl}_3$ )  $\delta$  0.99 (d,  $J = 6.5$ , 3H), 1.08 (ddd,  $J = 7.9$ , 10.6, 12.4, 1H), 1.22 (d,  $J = 6.2$ , 3H), 1.42 (dq,  $J = 11.4$ , 0.7, 3H), 1.46 (dq,  $J = 11.4$ , 0.7, 3H), 2.08 (m, 1H), 2.25 (m, 1H), 2.64 (dt,  $J = 9.3$ , 10.0, 1H), 3.33 (m, 1H), 3.71 (qddd,  $J = 6.2$ , 7.0, 7.9, 8.7, 1H);  $^{13}\text{C}$  NMR ( $\text{CDCl}_3$ )  $\delta$  15.5 (d,  $J = 45$ ), 16.4 (d,  $J = 45$ ), 17.1, 23.9 (2 signals), 34.9 (2 signals), 43.9 (2 signals), 53.6 (2 signals), 54.1 (2 signals); IR (neat) 1142, 1307, 1640  $\text{cm}^{-1}$ ; HRMS calcd  $\text{C}_8\text{H}_{18}\text{NOPNa}$   $m/z$  198.1024, found 198.1050. **(4, trans):**  $^1\text{H}$  NMR ( $\text{CDCl}_3$ )  $\delta$  1.00 (d,  $J = 6.5$ , 3H), 1.12 (d,  $J = 6.2$ , 3H), 1.42 (dq,  $J = 11.4$ , 0.7, 3H), 1.45 (dq,  $J = 11.4$ , 0.7, 3H), 1.53–1.68 (several peaks, 2H), 2.38 (m, 1H), 2.65 (m, 1H), 3.26 (ddd,  $J = 2.2$ , 7.3, 9.0, 1H), 3.79 (m, 1H);  $^{13}\text{C}$  NMR ( $\text{CDCl}_3$ )  $\delta$  13.7 (d,  $J = 45$ ), 15.0 (d,  $J = 45$ ), 17.4, 26.9 (2 signals), 32.2 (2 signals), 42.4 (2 signals), 53.4 (2 signals), 53.6 (2 signals);

IR (neat) 1142, 1307, 1640  $\text{cm}^{-1}$ ; HRMS calcd  $\text{C}_8\text{H}_{18}\text{NOPNa}$   $m/z$  198.1024, found 198.1050.

**Acknowledgment.** We thank the Swedish Research Council for financial support and the National Supercomputer Center at Linköping for generous allocation of computing time.

**Supporting Information Available:** General experimental, Cartesian coordinates, absolute energies, and  $\langle S^2 \rangle$  values for all reactant conformers and transition states. This material is available free of charge via the Internet at <http://pubs.acs.org>.

JO030294H